ACERP:Vol. 5, No.2, (Spring 2019) 6-11

Advanced Ceramics Progress

Research Article

Journal Homepage: www.acerp.ir

Characterization and Bioactivity of a Quaternary Phosphate-based Glass Powder Synthesized by Sol-Gel Method

Marzieh Jalilpour [a], Mohammad Rezvani * [a], Khalil Farhadi [b]

[a] *Department of Materials Science and Ceramics, University of Tabriz, Tabriz, Iran*
[b] *Faculty of Chemistry of Urmia University, Urmia, Iran*

PAPER INFO

Paper history:

Received 19 June 2019
Accepted in revised form 29 July 2019

Keywords:

Phosphate-based glass
Sol-gel
In vitro Bioactivity
Hydroxyapatite
Titanium Oxide
Ethanol

ABSTRACT

Phosphate-based glasses are suitable candidates for biomedical applications due to their porous structure. This study illustrates the properties and structural characterization of titanium-phosphate glass powders in the $55(P_2O_5)$-25(CaO)-(20-x)(Na_2O)-x(TiO_2), (x= 5, 10, 15) systems, which were prepared via sol-gel method. For this purpose, precursors of P_2O_5, CaO, Na_2O, and TiO_2 were added together dropwise on the magnetic stirrer after diluting or dissolving in ethanol. After gel formation, drying was done for various time periods at 60, 120, 180 and 200 °C. The structural and thermal properties of the obtained stabilized sol-gel glass powders were characterized using X-Ray Diffraction (XRD), Fourier Transform Infrared (FT-IR) spectroscopy, Simultaneous Thermal Analysis (STA), Brunauer-Emmett-Teller surface area, porosity analyzer (BET), and Scanning Electron Microscopy (SEM). The XRD results confirmed the amorphous and glassy nature of the prepared samples. FT-IR Spectroscopy results showed that the local structure of glasses changed with increasing TiO_2 content. As TiO_2 content increased in the glass structure, the phosphate connectivity increased. It was indicated that the addition of TiO_2 correlated unequivocally with an increase in glass stability. Also, to assess specimen's bioactivity, the samples were soaked in Simulated Body Fluid (SBF) for 7 days. The results of this study suggested that glass composition had a significant influence on apatite-forming ability, indicating the possibility to customize the properties of this class of materials towards the biomedical applications.

1. INTRODUCTION

Bioactive glasses are useful materials in the process of bone tissues regeneration because of their ability to bind the living bone when they are implanted in hard tissues [1]. In the early 1970s, Larry L Hench reported on the bone-bonding ability of the SiO_2-CaO-Na_2O-P_2O_5 glass system. This glass system is known as the Bioglass® [2]. Today a wide range of bioactive glass compositions have been developed through different synthesis routes and found a variety of applications including soft tissue bonding, lung tissue engineering, inducing angiogenesis, stimulating the gene expression, and growth factor production in osteoblasts [3-9].
Although the process of in vivo osseointegration of silica-rich glasses is well recognized, this bioactive performance can be reproduced using in vitro techniques through soaking the material in Simulated Body Fluid (SBF) in which, a new calcium phosphate phase is created on their surfaces [10]. However, due to the insolubility of the silica-rich glasses, they are only used as a component of long-term devices [1]. In contrast, calcium phosphate glasses that are currently studied can be prepared with a chemical composition analogous to the natural bone and therefore their solubility can be tailored to specific applications [11]. Different biocompatibility studies have demonstrated that these glasses do not produce adverse cell reactions on osteoblasts or fibroblasts [12, 13]. For these reasons, calcium phosphate glasses have a great potential in the development of degradable devices, as well as, in the building of temporary scaffolds intended to support the regeneration of hard tissues [14, 15]. In order to control the solubility of calcium phosphate glasses in humid

*Corresponding Author Email: m_rezvani@tabrizu.ac.ir (M. Rezvani)

environments, ions such as Fe^{+3}, Al^{+3}, Zn^{+2}, and Ti^{+4} have been used in novel glass formulations [16-19]. Phosphate-based glasses containing ions which are routinely found in the human body, (such as Ca^{2+} and Na^{+}) can be classed as bioresorbable and biocompatible. They have predictable dissolution rates which can be controlled by varying the composition and being entirely amorphous. Their dissolution is relatively uniform and there is little risk of residual fragments causing sterile inflammation. Calcium phosphate deposition is well recognized from in vitro and in vivo studies. It is established that the mechanism of hydroxyapatite (HA) formation involves the dissolution of Ca^{+2} ions from the surface of bioactive materials, which increases the saturation in the surrounding fluid with respect to HA components [20].
Among the several glass synthesis methods [21], the melt-quenching and sol-gel are most popular. The sol-gel has some advantages over traditional melt-quenching approaches in biomedical applications; the most notable of which are preparation at low temperatures which allows scope for the encapsulation of drugs into the biomaterial, and the potential to coat biomedical devices using sol-gel processing to improve their properties, e.g. a hydroxyapatite layer to improve bonding to bone [22].
Considering this fact that Ti ions have an important role in formation and degradation rate of glass, in the present work the effect of the TiO_2 content on quaternary phosphate-based sol-gel derived glass powders was analyzes in the P_2O_5-CaO-Na_2O-TiO_2 system. For this purpose, ethanol was used as the solvent for the first time in this system. Analyzing was mainly done by X-ray diffraction (XRD), thermal analysis (TG and DTA), Fourier transform infrared (FT-IR) spectroscopy, scanning electron microscopy (SEM), Brunauer-Emmett-Teller (BET), and Barrett-Joyner-Halenda (BJH). A preliminary study on in vitro bioactive behavior of phosphate glass was also carried out by immersion in SBF. Then, the samples were analyzed by XRD, FT-IR and SEM to investigate the hydroxyapatite formation.

2. MATERIALS AND METHODS

2.1. Materials

The following chemical precursors were used without further purification; Triethyl Phosphate (Sigma Aldrich, USA, ≥99.8% purity), Titanium Isopropoxide (Merck, Germany, 97% purity), Calcium Nitrate tetrahydrate (Merck, ≥99.7 purity, %30 wt% in ethanol), sodium ethoxide solution (Sigma Aldrich, USA, ≥95 % purity, 30 wt% in ethanol), ethanol (Merck, Germany, ≥99.7% purity) and Dimethylformamide (DMF) (Merck, Germany, 99.8% purity).

2.2. Synthesis of the Glasses

First, the triethyl phosphate was diluted in ethanol in a molar ratio of 1:3 and allowed to react for 15 min (the whole reaction was carried out in a dried vessel in closed reflux system). Then titanium isopropoxide was added to the mixture drop by drop while it was magnetically stirring. After 1h of stirring, calcium nitrate tetra hydrate solution (30 wt% in ethanol) was added dropwise into the vessel. Stirring was continued for 1h and then, sodium ethoxide solution (30 wt% in ethanol) was added gradually and stirred for 1h. In the last step of the synthesis process, DMF was added to the solution and the solution was stirred for 30 min. For all samples, the mixture poured into the porcelain crucible and allowed until the gel formed. The mixtures were aged for 3 days at room temperature. Following the aging stage, the temperature was increased to 60 °C and held for 2 days, and then to 120 °C for 2 more days. Then, the samples were dried at 180 °C for 2 days and then at 220 °C for 2h. In the last step of drying, any remaining solvent was removed and semi-bulk samples were obtained. The samples containing 5, 10 and 15% TiO_2 were named Eth_5, Eth_{10} and Eth_{15}; respectively. Details related to the code and the compositions of the three glasses are presented in Table 1.

TABLE 1. Compositions (mol%) of the sol-gel glasses

Glass code	Glass Composition	Concentration (mol %)			
		P_2O_5	CaO	Na_2O	TiO_2
Eth_5	55P_2O_5-25CaO-15Na_2O-5TiO_2	55	25	15	5
Eth_{10}	55P_2O_5-25CaO-10Na_2O-10TiO_2	55	25	10	10
Eth_{15}	55P_2O_5-25 CaO-5Na_2O-15TiO_2	55	25	5	15

2.3. Characterization of the glass powder

The XRD patterns of fine glass powders (poured in flat plate geometry) were obtained by a Philips Diffractometer (PHILIPS PW1730, Netherland) using Ni filtered Cu Kα radiation. Data was collected using a Lynx Eye detector with a step size of 0.05° over an angular range of 2θ = 10-80°.
Differential thermal analysis (Bahr STA 504, Germany) was conducted to identify the glass transition (T_g) and crystallization temperatures (T_c) of samples. Analysis was carried out on powdered glass samples in an alumina crucible in a range temperature from 25 to 800 ºC at a heating rate of 10 ºC/min under air atmosphere. An alumina (Al_2O_3) crucible was used as a reference. The thermogravimetric analysis (TGA) was used to quantify the total weight loss of the samples.

The glass powders were characterized by infrared spectroscopy (NEXUS 670, USA). About 10 mg of each sample was blended with KBr (Sigma-Aldrich) (1:100) for IR spectroscopy and then pressed into translucent pellets for the measurement. Spectra were obtained at range of 4000-400 cm^{-1}.

The morphology and grain size of the synthesized glasses were determined by electron microprobe analyses. After coating by gold, the samples were analyzed in the field emission scanning electron microprobe (FE-SEM) (TSCAN, Mira3LMU, Czech Republic) to determine morphology and grain size before and after soaking in SBF.

Textural characterization was conducted by using gravimetric nitrogen Brunauer-Emmett-Teller (BET) surface analysis technique, using a Micrometrics ASAP 2020 Micro pore Analyzer (Micrometrics, Norcross, GA). The pore volume, average pore diameter and pore size distribution were calculated from the adsorption branches of the isotherms using the Barrett-Joyner-Halanda (BJH) method.

The bioactivity of the glass powders was studied by soaking the samples in SBF. Five mg of glass powders were exposed to 25 mL of fresh solutions of SBF prepared using the Kokubo's protocol under human body condition (static conditions) at 37 ± 0.5 ºC during 7 days [10]. The solution was not replaced during the assay. After exposure, samples were washed off with ethanol and dried at room temperature for 24 h. The samples after soaking in SBF were named as S-Eth_5, S-Eth_{10} and S-Eth_{15} respectively.

The morphology of the hydroxyapatite formed on the surface of the samples was studied by Scanning Electron Microscopy. Also, the samples were characterized by Fourier-Transformed Infrared spectroscopy (FT-IR) and X-ray diffraction (XRD). After soaking in SBF, the samples were named S-Eth_5, S-Eth_{10} and S-Eth_{15}.

3. RESULTS AND DISCUSSION

Figure 1 (a and b) depicts the XRD spectra of sol-gel derived samples before and after soaking in SBF. A broad peak at 2θ=20-40° was observed in all compositions before soaking in SBF that was free from any detectable crystalline phase which confirmed the amorphous nature of the glasses (Figure 1a). After 7 days of soaking in SBF, as observed in the XRD patterns (figure 1b), characteristic peaks corresponding to hydroxyapatite (ICDD - PDF2 card: 00-009-0432) [23] appeared in all samples. The bioglass containing 5% TiO_2 demonstrated rather sharper peaks than other compositions. It was obvious that by increasing TiO_2 content to 15 %, the intensity of the hydroxyapatite peaks decreased slightly that can be due to decreasing the glass degradation rate and its solubility because of increasing phosphate bonds [24, 25]. It might also occur because of the decrease in the specific surface area of the samples by increasing the TiO_2 content, which limited the hydroxyapatite forming ability.

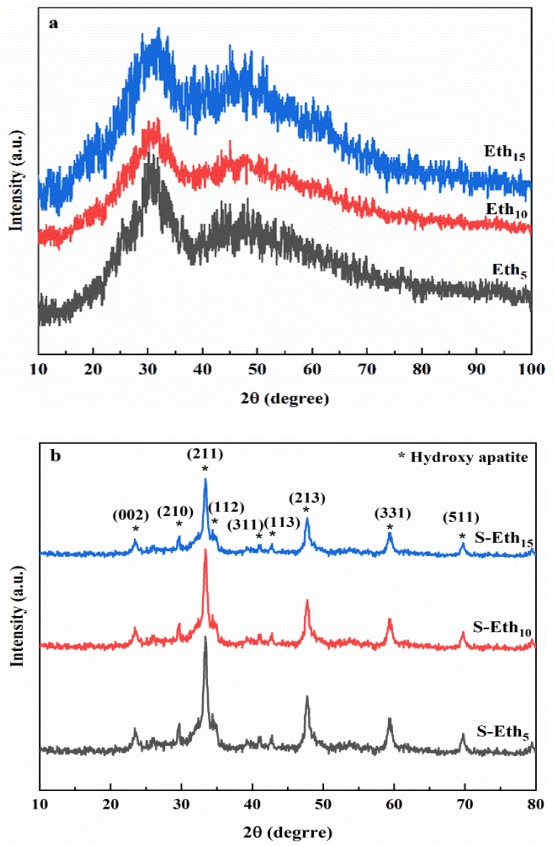

Figure 1. XRD spectra of sol-gel derived glasses containing 5, 10 and 15 % mol TiO_2, a) before and b) after 7 days of soaking in SBF

The FT-IR spectra of the three glass samples, before and after soaking in SBF for 7 days, are shown in Figure 2. The absorption bands were assigned according to other studies of phosphate-based glasses using infrared spectroscopy [26-29].

The spectra of the sol-gel samples exhibited the bands characteristic of P-O-P bonding at ~550-580, ~740 cm^{-1} and ~870-925 cm^{-1}, indicating that a significant number of these bonds were formed during the sol-gel reaction. The symmetric $(PO_3)^{-2}$ stretching mode , and the asymmetric $(PO_3)^{-2}$ vibrations were appeared at ~1054 cm^{-1} and 1116 cm^{-1}, respectively. The asymmetric vibrations at 1384-1420 cm^{-1} in the spectra of the sol-gel samples were indicative of the presence of $(CO_3)^{-2}$, whereas the bands at ~3420 and 1640 cm^{-1} were due to the presence of hydroxyl groups and the adsorbed moisture [30]. Increases in the intensity of the peaks at ~900 and ~1000 cm^{-1} were correlated with the

increasing substitution of sodium with titanium. It was due to the cross-linking effect of titanium that increased the polymerization of the phosphate network [31]. There was an obvious difference between the spectra of the Eth_5 and Eth_{15} due to the increase in phosphate bands due to increase in Ti content. The intensity of the bands at 1600 and 3400 cm^{-1} was significantly reduced in the spectra of Eth_5 and Eth_{15} by increasing the Ti content, providing further evidence that residual organic component and hydroxyls were driven off because of increasing in cross-linking.

The FT-IR spectra of the samples after 7 days of soaking in SBF presented a relatively sharp stretching band at 3415-3430 cm^{-1} which was related to hydroxyl ions. As usual for precipitated coatings, the bending mode band of H_2O was observed at ~1649 cm^{-1}. Some small bands associated with C-H stretching mode were observed at ~2190 cm^{-1} and 2338-2345 cm^{-1} that indicated the presence of some residual organic materials [31]. A phosphate band related to the P-O asymmetric stretching mode of the $(PO_3)^{-2}$ groups were found in the region from 1133 to 1149 cm^{-1}. Two other small bands at 1041 and 1056 cm^{-1} were associated with symmetric stretching $(PO_3)^{-2}$ and asymmetric stretching mode of the $(PO_4)^{-3}$, respectively [29, 31]. The bands at 1438 cm^{-1}, 1445 cm^{-1}, and 1452 cm^{-1} are associated to $(CO_3)^{-2}$ group of carbonated apatite. These bands are difficult to form which indicate that the content of $(CO_3)^{-2}$ bands is low [1]. This is the reason for the formation of hydroxyapatite. However, the characteristic peaks at ~920-1100 cm^{-1} indicated the presence of HPO_4^{-2} in the crystal lattice [1]. The presence of sharper $(PO_4)^{-3}$ bond in the FT-IR spectrum of Eth_{10} confirmed the better hydroxyapatite forming ability in this sample compared to the Eth_5. The bands at 739 cm^{-1} and ~559-574 cm^{-1} could be associated with P-O-P symmetric stretching and symmetric stretching band, respectively. The results indicated that the proper Ca/P ratio was most likely formed in the hydroxyapatite by low content of carbonate. The presence of HPO_4^{-2} could indicate a deficiency of carbonate in the newly formed coating [1, 31].

Simultaneous thermal analysis (STA) of the Eth_{10} was carried out to determine the correct heat treatment temperature. Two obvious stages of weight loss on the TGA curve were observed (Figure 3). First, the mass loss occurred between 60 °C and 320 °C, attributed to an endothermic reaction at 106 °C. The removal of physically adsorbed water and solvents caused the mass loss of about 12% wt. The second weight loss commenced from 320 °C to about 800 °C. It correlated to a small endothermic and a rather broad exothermic peak in the DTA curve. At 654 °C, glass transition occurred as an endothermic and crystallization of glass powder occurred at around 739 °C as an exothermic peak, respectively. Also, a spread peak was observed at 390 °C due to the loss of alkoxy groups [32]. This weight loss was about 12wt %, too.

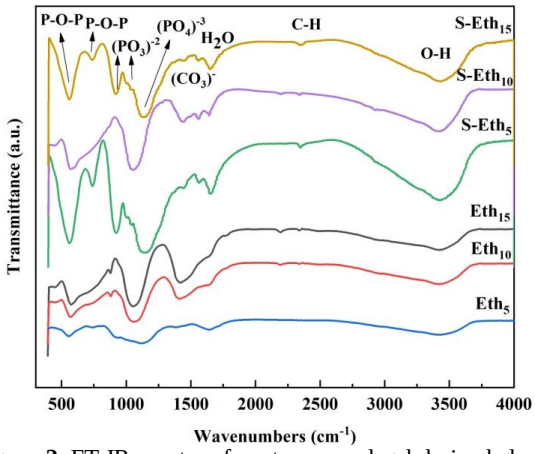

Figure 2. FT-IR spectra of quaternary sol-gel derived glasses containing 5, 10, 15 % mol TiO_2, before and after soaking in SBF for 7 days

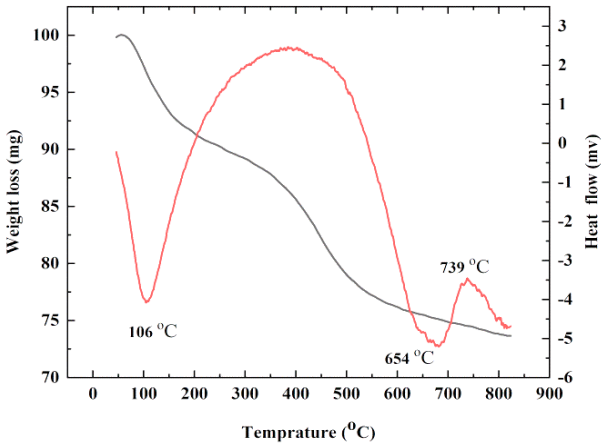

Figure 3. Simultaneous TGA and DTA measurements of the $55P_2O_5$-25CaO-$10Na_2O$-$10TiO_2$ glass powder

Specific surface area, average pore diameter, and total pore volume of Eth_{10} were measured and the results are summarized in Table 2. The sample was degassed at 200°C for 2 h in flowing nitrogen before the BET-BJH measurements. The adsorption isotherm and pore size distribution diagram of the sample are shown in Figure 4a and 4b; respectively. The specific surface area obtained from the adsorption isotherms of Eth_{10} was about 81m^2/g. This surface area is suitable for many biomedical applications [33].

The adsorption isotherm curve of Eth_{10} was identified as the type IV isotherms that show characteristic of mesoporous materials. The obtained hysteresis loop was H_1 type in the mesopore range, which is the characteristic of cylindrical pores open on both sides [34].

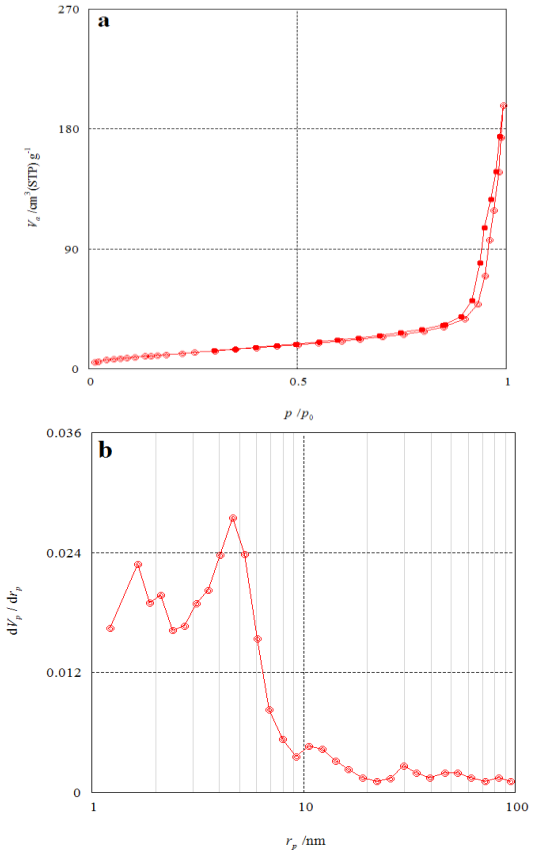

Figure 4. a) adsorption isotherm and b) pore distribution diagram of Eth_{10}

TABLE 2. Specific surface area, average pore diameter, and total pore volume of Eth_{10}

Sample name	Eth_{10}
specific surface area (m^2/g)	80.88
total pore volume (cm^3/g)	0.2833
average pore diameter (nm)	14.014
pore radian peak (nm)	4.62

SEM images of Eth_{10} bioactive glass nanopowder, before and after soaking in SBF for 7 days, are shown in Figure 5a and 5b, respectively. It is interesting to see that the morphology of particles was spherical, and their sizes were smaller than 50 nm (mean particle size of glass powder was about 20 nm (figure 5a). However, sever agglomeration was observed in the glass powder due to its fine size which was relevant to the method that the bioglasses were synthesized from it. Figure 5b shows the surface of the Eth_{10} after soaking in SBF solution. Compared to Figure 5a, it is clear that the hydroxyapatite particles formed on the surface of glass powder (as shown in XRD pattern and FT-IR spectrum) [35]. The mean particle size of hydroxyapatite was about 8 nm with a spherical morphology.

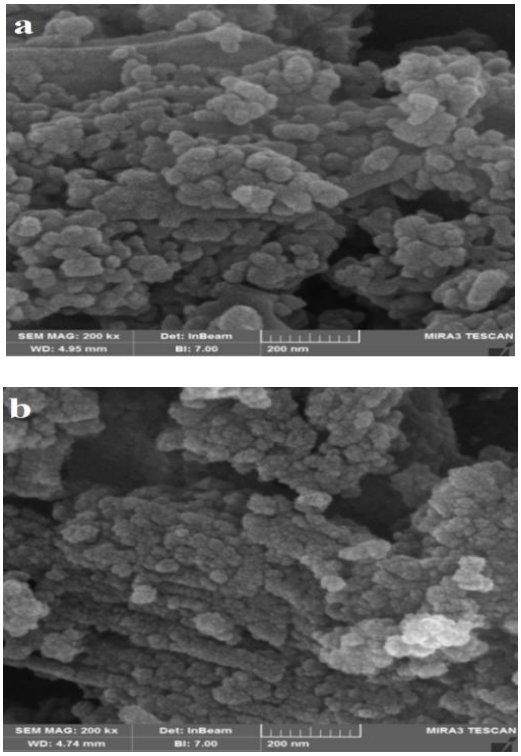

Figure 5. SEM images of Eth_{10} glass powder a) before and b) after soaking in SBF for 7 days

4. CONCLUSION

In the present work, quaternary phosphate-based glass powders containing 5, 10, and 15 mol% TiO_2 were successfully synthesized via a facile and low-temperature sol-gel method. The high surface area and good degradation ability phosphate-based glasses had a significant effect on hydroxyapatite formation. The substitution of Na_2O with 5 or 10 mol% TiO_2 improved nano spherical hydroxyapatite formation. So, it can be concluded that the synthesized glass powders have a good potential to be used in biomedical applications.

5. ACKNOWLEDGMENTS

The authors would like to acknowledge the support of the Institute of nanotechnology and biotech center of Urmia University for this research.

6. REFERENCES

1. Alonso L. M., Garcıa-Menocal J. A. D., Aymerich M. T., Guichard J. A. A., Garcıa-Valles M., Manent S. M., Ginebra M., "Calcium phosphate glasses: Silanation process and effect on the bioactivity behavior of Glass-PMMA composites", ***Journal of biomedical materials research B: applied biomaterials***, Vol. 00B, (2013), 1-9.

2. Mukundan L. M., Nirmal R., Vaikkath D., Nair P. D., "A new synthesis route to high surface area sol-gel bioactive glass through alcohol washing", ***Biomaterials***, Vol. 3, No. 2, (2013), e24288; 1-10.
3. Wilson J., D. Nicolletti, Yamamuro T., Hench L. L., Wilson J., "Bonding of soft tissues to bioglass. In: Handbook of bioactive ceramics: bioactive glasses and glass-ceramics", ***Boca Raton FL: CRC Press***, (1990), 283-302.
4. Wilson J., Pigott G. H., Schoen F. J., Hench L. L., "Toxicology and biocompatibility of bioglasses", *Journal of biomedical materials research*, Vol. 15, (1981), 805-817.
5. Tan A., Romanska H. M., Lenza R., Jones J., Polak J. M., Bishop A. E., "The effect of 58S bioactive sol-gel derived foams on the growth of murine lung epithelial cells", ***Key Engineering Materials***, Vol. 240, No. 242, (2003), 719-724.
6. Verrier S., Blaker J. J., Maquet V., Hench L. L., Boccaccini A. R., "PDLLA/Bioglass composites for soft-tissue and hard-tissue engineering: an in vitro cell biology assessment", ***Biomaterials***, Vol. 25, (2004), 3013-3021.
7. Day R. M., "Bioactive glass stimulates the secretion of angiogenic growth factors and angiogenesis in vitro", ***Tissue Engineering***, Vol. 11, (2005), 768-777.
8. Xynos I. D., Edgar A. J., Buttery L. D. K., Hench L. L., Polak J. M., "Gene-expression profiling of human osteoblasts following treatment with the ionic Products of Bioglass 45S5 dissolution", ***Journal of biomedical materials research***, Vol. 55, (2001), 151-157.
9. Xynos I. D., Edgar A. J., Buttery L. D., Hench L. L., Polak, J. M., "Ionic dissolution products of bioactive glass increase proliferation of human osteoblasts and induce insulin-like growth factor II mRNA expression and protein synthesis", ***Biochemical* and *Biophysical Research Communications***, 276: 2000, 461-465.
10. Kokubo T., Takadama H., "How useful is SBF in predicting in vivo bone bioactivity?", ***Biomaterials***, Vol. 27, (2006), 2907-2915.
11. Ahmed I., Lewis M., Olsen I., Knowles J. C., "Phosphate glasses for tissue engineering, Part 1. Processing and characterization of a ternary-based P_2O_5-CaO-Na_2O glass system", ***Biomaterials***, Vol. 25, (2004), 491-499.
12. Navarro M., Ginebra M. P., Planell J. A., "Cellular response to calcium phosphate glasses with controlled solubility", ***Journal of biomedical materials research A***, Vol. 67, (2003), 1009-1015.
13. Bitar M., Salih V., Mudera V., Knowles J. C., Lewis M. P., "Soluble phosphate glasses: In vitro studies using human cells of hard and soft tissue origin", ***Biomaterials***, Vol. 25, No. 12, (2004), 2283-2292.
14. Franks K., Abrahams I., Knowles J. C., "Development of soluble glasses for biomedical use. I. In vitro solubility measurement", ***Journal of Materials Science: Materials in Medicine***, Vol. 11, (2000), 609-614.
15. Navarro M., Del Valle S., Ginebra M. P., Martınez S., Planell J. A., "Development of new calcium phosphate glass ceramic porous scaffold for guided bone regeneration", ***Key Engineering Materials***, (2004), 254-256, 945-948.
16. Simon V., Muresan D., Simon S., "Iron effect on glass stability of sodium-calcium-phosphate glasses", ***European Physical Journal-Applied Physics***, Vol. 37, (2007), 219-222.
17. Banijamali S., Eftekhari Yekta B., Aghaei A. R., "Self-patterning of porosities in the CaO-Al_2O_3-TiO_2-P_2O_5 glass-ceramics via ion exchange and acid leaching process", ***Journal of Non-Crystalline Solids***, Vol. 380, (2013), 114-122.
18. Abou Neel E. A., O'Dell L. A., Smith M. E., Knowles J. C., "Processing, characterization, and biocompatibility of zinc modified metaphosphate based glasses for biomedical applications", ***Journal of Materials Science: Materials in Medicine***, Vol. 19, (2008), 1669-1679.
19. Navarro M., Ginebra M. P., Clement J., Martınez S., Avila G., Planell J. A., "Physicochemical degradation of titania-stabilized soluble phosphate glasses for Medical applications", ***Journal of American Ceramic Society***, Vol. 86, (2003), 1345-1352.
20. Clement J., Manero J. M., Planell J. A., Avila G., Martınez S., "Analysis of structural changes of a phosphate glass during its dissolution in simulated body fluid", ***Journal of Materials Science: Materials* in *Medicine***, Vol. 10, (1999), 729-732.
21. Sharifianjazi F., Parvin N., Tahriri M., "Synthesis and characteristics of sol-gel bioactive SiO_2-P_2O_5-CaO-Ag_2O glasses", ***Journal of Non-Crystalline Solids***, (2017), 108-113.
22. Pickup D. M., Valappil S. P., Moss R. M., Twyman H. L., 'Guerry P., Smith M. E., Wilson M., Knowles J. C., Newport R. J., "Preparation, structural characterisation and antibacterial properties of Ga-doped sol-gel phosphate-based glass", ***Journal of Materials Science***, Vol. 44, No. 7, (2009), 1858-1867.
23. Ungureanu D. N., Angelescu N., Bacinschi Z., Valentina Stoian E., Rizescu C. Z., "Thermal stability of chemically precipitated hydroxyapatite nanopowders", ***International Journal of Biology and Biomedical Engineering***, Vol. 5, No. 2, (2011), 57-64.
24. Foroutan F., De Leeuw N. H., Martin R. A., Palmer G., Owens G. J., Kim H. W., Knowles J. C., "Novel sol-gel preparation of $(P_2O_5)_{0.4}$-$(CaO)_{0.25}$-$(Na_2O)_X$-$(TiO_2)_{(0.35-X)}$ bioresorbable glasses (X = 0.05, 0.1, and 0.15)", ***Journal of Sol-Gel Science and Technology***, Vol. 73 (2), (2015), 434-442.
25. Brauer D. S., Rüssel C., Li W., Habelitz S., "Effect of degradation rates of resorbable phosphate invert glasses on in vitro osteoblast proliferation", ***Journal of Biomedical Materials Research: Part A.***, Vol. 77A (2), (2006), 213-219.
26. Kim D. S., Shin J. Y., Ryu B. K., "Proton Conduction in and Structure of P_2O_5-TiO_2-CaO-Na_2O Sol-Gel Glasses", ***Journal of the Korean Physical Society***, Vol. 70, No. 12, (2017), 1054-1059.
27. Arsad Maisara S. M., Pat M. L., "Synthesis and Characterization of hydroxyapatite Nanoparticles and β-TCP Particles", ***2nd International Conference on Biotechnology and Food Science***, Vol. 7, (2011), 184-188.
28. Davim E. J. C., Fernandes M. H. V., Senos A. M. R., "Increased surface area during sintering of calcium phosphate glass and sodium chloride mixtures", ***Journal of the European Ceramic Society***, Vol. 35, (2015), 329-336.
29. Solgi S., Shahrezaee M., Zamanian A., Jafarzadeh Kashi T. S., Raz M., Khoshroo K., Tahriri M., "Sol-gel synthesis and characterization of SiO_2-Cao-P_2O_5-SrO bioactive glass: in vitro study", ***Key Engineering Materials***, Vol. 631, (2015), 30-35.
30. Pickup D. M., Guerry P., Moss R. M., Knowles J. C., Smith M. E., Newport R. J., "New sol-gel synthesis of a $(CaO)_{0.3}(Na_2O)_{0.2}(P_2O_5)_{0.5}$ bioresorbable glass and its structural characterization"", ***Journal of Materials Chemistry***, Vol. 17, (2007), 4777-4784.
31. Foroutan F., Walters N. J., Owens G. J., Mordan N. J., Kim H. W., Leeuw N. H., Knowles J. C., "Sol-gel synthesis of quaternary $(P_2O5)_{55}$-$(CaO)_{25}$-$(Na_2O)_{(20-x)}$-$(TiO_2)_x$ bioresorbable glasses for bone tissue engineering applications (x = 0, 5, 10, or 15)", ***Biomedical Material***, Vol. 10, No. 045025, (2015), 1-11.
32. Solgi S., Khakbiz M., Shahrezaee M., Zamanian A., Tahriri M., Keshtkari S., Raz M., Khoshroo K., Moghadas S., Rajabnejad A., "Synthesis, Characterization and In Vitro Biological Evaluation of Sol-gel Derived Sr-containing Nano Bioactive Glass", ***Silicon***, Vol. 9, No. 5, (2017), 535-542.
33. Masel R. I., Principles of adsorption and reaction on solid surfaces. Wiley, New York, (1996).
34. Lowell S., Shields J. E., Thomas M. A., Thommes M., "Characterization of Porous Solids and Powders: Surface Area, Pore Size and Density", Kluwer Academic Publisher, Dordrecht, (2006), 12-15.
35. Montazerian M., Eftekhari Yekta B., Marghussian V. K., Bellani C. F., Siqueira R. L., Zanotto E. D., "Bioactivity and cell proliferation in radiopaque gel-derived CaO-P_2O_5-SiO_2-ZrO_2 glass and glass-ceramic powders", ***Materials Science and Engineering C***, Vol. 55, (2015), 436-447.